This is the accepted version of the following article: "High Tc superconductivity at the interface between the CaCuO2 and SrTiO3 insulating oxides", which has been published in final form on Physical Review Letters at https://journals.aps.org/prl/abstract/10.1103/PhysRevLett.115.147001; DOI: 10.1103/PhysRevLett.115.147001

High T_c superconductivity at the interface between the $CaCuO_2$ and $SrTiO_3$ insulating oxides

D. Di Castro[1,2,*], C. Cantoni[3], F. Ridolfi[1], C. Aruta[2], A. Tebano[1,2], N. Yang[2,4], G. Balestrino[1,2]

[1]*Dipartimento di Ingegneria Civile e Ingegneria Informatica, Università di Roma Tor Vergata, Via del Politecnico 1, I-00133 Roma, Italy*

[2]*CNR-SPIN, Università di Roma Tor Vergata, Roma I-00133, Italy*

[3]*Materials Science and Technology Division, Oak Ridge National Laboratory, Oak Ridge, TN 37831-6116, USA*

[4]*Facoltà di Ingegneria, Università degli studi Niccolò Cusano, Rome I-00166, Italy*

*daniele.di.castro@uniroma2.it

Abstract

At interfaces between complex oxides it is possible to generate electronic systems with unusual electronic properties, which are not present in the isolated oxides. One important example is the appearance of superconductivity at the interface between insulating oxides, although, until now, with very low T_c. We report the occurrence of *high* T_c superconductivity in the bilayer $CaCuO_2/SrTiO_3$, where both the constituent oxides are insulating. In order to obtain a superconducting state, the $CaCuO_2/SrTiO_3$ interface must be realized between the Ca plane of $CaCuO_2$ and the TiO_2 plane of $SrTiO_3$. Only in this case extra oxygen ions can be incorporated in the interface Ca plane, acting as apical oxygen for Cu and providing holes to the CuO_2 planes. A detailed hole doping spatial profile has been obtained by STEM/EELS at the O K-edge, clearly showing that the (super)conductivity is confined to about 1-2 $CaCuO_2$ unit cells close to the interface with $SrTiO_3$. The results obtained for the $CaCuO_2/SrTiO_3$ interface can be extended to multilayered high T_c cuprates, contributing to explain the dependence of T_c on the number of CuO_2 planes in these systems.

The layered structure of cuprate high T_c superconductors (HTS) can be schematized as a sequence of natural interfaces between two different blocks: an insulating block with “infinite layers” (IL) structure, i.e., containing a sequence of CuO_2 planes and Ca planes stacking along the c-axis, and a charge reservoir (CR) block, that, opportunely doped by chemical substitution or excess oxygen ions,

provides charge carriers to the IL block. The extraordinary electronic properties shown by the interface between two insulating oxides [1-8], as the LAO/STO interface [2,4,9], which is even superconducting at ~ 10^{-1} K [4,9], suggested the opportunity to exploit conducting interface as a charge reservoir to dope a cuprate with IL structure, and thus to dramatically raise the T_c from ~ 10^{-1} K to ~ 10^{2} K. We recently explored such a possibility by tailoring artificial high T_c superconducting superlattices $[(CaCuO_2)_n/(SrTiO_3)_m]_N$ (T_c = 50 K), made by N repetitions of the $(CaCuO_2)_n/(SrTiO_3)_m$ bilayer, where n and m are the number of unit cells of IL $CaCuO_2$ (CCO) and $SrTiO_3$ (STO), respectively [6,10]. Indeed, it has been shown that the tetragonal phase of CCO, with $a = b = 3.86$ Å and $c = 3.20$ Å, can be stabilized in form of thin film by the good lattice match with perovkite substrates, in particular with $NdGaO_3$ [11]. The tetragonal phase shows an IL structure as in the IL block of HTS. Therefore, CCO is considered the parent compound of HTS with the simplest lattice structure. Differently from previous cuprate/cuprate heterostructures [5,12,13], now the spacer between the superconducting blocks is not a cuprate, but STO. The CCO/STO interfaces are thus very similar to the IL/CR native interface in HTS. The results obtained from the investigation of the CCO/STO interface can be used to extract important information on the physical processes occurring in HTS.

In this work, by using state-of-the-art aberration-corrected scanning transmission electron microscopy (STEM) coupled to electron energy loss spectroscopy (EELS), we investigate the CCO/STO interface in the bilayer $(CCO)_n/(STO)_m$, with unprecedent spatial resolution [14]. We find that this interface shows high T_c superconductivity, with optimal T_c about 40 K. We give *direct* evidence that doping holes are provided by the introduction of extra oxygen ions at the CCO/STO interface and are confined within 1-2 CCO unit cells.

We used the pulsed laser deposition technique [14] to synthesize the CCO/STO bilayers on NdO terminated $NdGaO_3$ (NGO) substrates. A detailed structural characterization of the large number of CCO/STO heterostructures grown has been obtained by X-Ray Diffraction and STEM measurements [14].

As in CCO/STO superlattices [6], the conductivity, and thus the T_c, of CCO/STO bilayers vary substantially with varying the oxidizing power of the growth atmosphere, from an insulating to a superconducting behaviour. On the other hand, in bare CCO films no superconducting phase has been

revealed at any oxidizing growth conditions. This finding clearly indicates that the interface with the STO is the structural feature needed for the occurrence of superconductivity. Since in the superlattices each CCO block is embedded between two STO blocks, two kinds of interface structures are present, at the top and at the bottom side of the CCO: CuO_2-Ca-TiO_2-SrO and TiO_2-SrO-CuO_2-Ca, respectively, which could behave differently.

The bilayer CCO/STO grown on NdO-terminated NGO substrate gives us the possibility to discriminate between the two kinds of interfaces (see Fig. 1). Indeed, if the CCO is deposited first (NGO/CCO/STO heterostructure), the CCO/STO interface presents the following sequence of atomic planes: CuO_2-Ca-TiO_2-SrO (see Fig.1b), which we call interface α. On the other hand, if STO is deposited first (NGO/STO/CCO heterostructure), the interface between STO and CCO is TiO_2-SrO-CuO_2-Ca (see Fig.1c), which we call interface β. The two different atomic plane sequences have been confirmed by STEM, as shown below. In Fig.1a we report the R(T) curves for the two samples with different stacking order: only the NGO/CCO/STO system is superconducting. From these findings we deduce that, most probably, only the interface α is capable to host superconductivity (see Fig.1b).

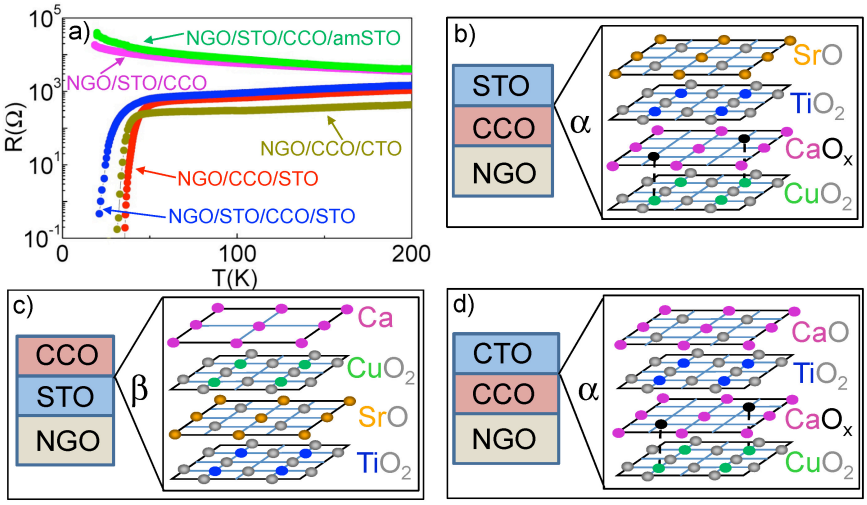

Figure 1: a) R(T) for NGO/CCO/STO, NGO/CCO/CTO, NGO/STO/CCO, NGO/STO/CCO/STO, and NGO/STO/CCO/amSTO with the top amorphous STO (amSTO) layer. b)-d) Schematic interface structures for the bilayers NGO/CCO/STO (b), NGO/STO/CCO (c) and NGO/CCO/CTO (d). The extra oxygen ions introduced in the Ca plane at the interface in NGO/CCO/STO and NGO/CCO/CTO are shown in black togheter with the corresponding apical coordination with the Cu ions (dashed black line).

This hypothesis has been further checked by growing a trilayer NGO/STO/CCO/STO. Here, both α and β interfaces are present and the superconducting behaviour is recovered (see Fig.1a). Moreover, if the top STO layer in the trilayer is made of amorphous STO (grown at low temperature), the system remains insulating (Fig.1a). This confirms that a sharp, crystalline CuO_2-Ca-TiO_2-SrO interface is necessary for superconductivity. Previous bulk-sensitive measurements on CCO/STO superlattices have suggested that charge doping results from extra oxygen atoms which are introduced in the system during the growth, most probably at the CCO/STO interfaces [6,10,15,16]. In agreement with this hypothesis, we note that, when the Ca plane faces to the TiO_2 plane in the CuO_2-Ca-TiO_2-SrO α interface, it can host extra oxygen ions giving rise to a CaO_x plane, as indicated by the black dots in Fig.1b. Every extra apical oxygen ion can inject two holes in the lower lying CuO_2 planes, thus inducing superconductivity. In the interface β, the SrO plane is already stoichiometrically full of oxygen ions (Fig.1c), and no hole doping can occur.

To experimentally check this hypothesis, we performed aberration-corrected STEM/EELS measurements on both kinds of interfaces in different regions of the same sample and on different samples, obtaining similar results. In Fig.2, we show STEM images of the CCO/STO interface of NGO/$(CCO)_9$/$(STO)_{55}$, where the α interface is present. The images are acquired simultaneously using both the annular bright field (ABF) detector, which is sensitive to scattering from light O atoms (panel a), and the high-angle annular dark field (HAADF) detector, which yields Z-contrast and is preferred for imaging the heavier cations (panel b) [14]. Because in ABF imaging the atoms appear dark on a light background, the ABF image in Fig. 2a has been inverted in order to show the atoms as bright spots on a dark background. In order to better visualize both cations and oxygen columns, an overlay of the HAADF image colored in red and the inverted ABF image colored in green is shown in Fig. 2c. In the overlay all the cations appear yellow/orange while the O shows up in green.

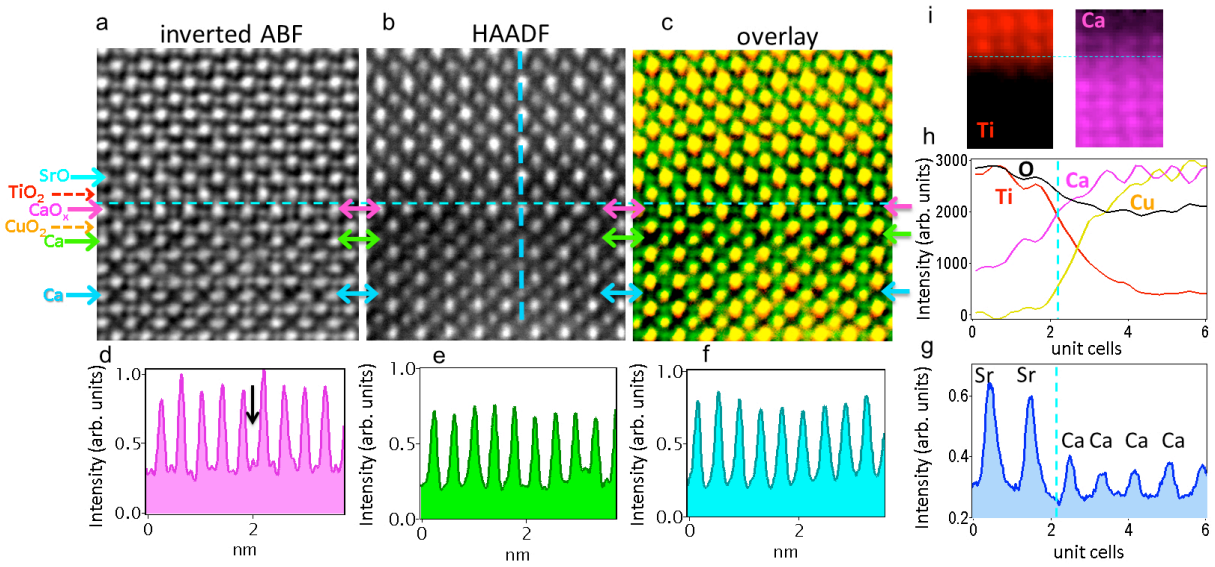

Figure 2: Structure of interface α in NGO/CCO/STO bilayer: a) Inverted ABF images showing O columns. b) HAADF image showing cations with Z contrast. c) overlay of (a) in green and (b) in red, showing all the cations in orange and the O columns in green. d), e), and f) are line profiles of the inverted ABF image at the magenta (interface Ca plane), green and blue arrow, respectively. The black arrow in d) indicates the intensity from oxygen columns in the interfacial CaO_x plane. h) EELS elemental profiles. g) intensity profile of the HAADF image (taken from the dashed blue line in b)). i) EELS elemental maps for Ti and Ca. Dashed cyan lines indicate the interface.

The intensity profiles of the inverted ABF image, taken at the first (panel d), second (panel e), and fourth (panel f) Ca planes indicate that a substantial amount of extra oxygen atoms are present only in the Ca plane at the interface with the TiO_2, thus forming a CaO_x plane, whereas no extra oxygen is detected in the fourth Ca plane. This result reveals that the charge reservoir role is played by a *single* atomic plane at the interface. The introduction of excess oxygen atoms only in the Ca plane at the interface with STO and not in the inner Ca planes can be explained by the presence of strain confined at the interface, together with the hybrid nature of the CCO/STO interface. Indeed, depending on the oxygen content x, the interface CaO_x plane can either couple with the CuO_2 plane below to form the infinite layer structure $CaCuO_2$, for the extreme case $x = 0$, or couple with the TiO_2 plane above to form the perovskite structure $CaTiO_3$, for the other extreme case $x = 1$, the latter being a stable compound in form of film. This opportunity makes the interface Ca plane unique with respect to the inner Ca planes of the CCO.

From the elemental maps and profiles obtained by EELS and shown in Fig. 2i and 2h the presence of some Ca/Sr interdiffusion at the interface is evinced. However, the occurrence of Ca/Sr

interdiffusion is not relevant for the appearance of superconductivity for two main reasons: 1) Ca is isovalent to Sr, therefore no Sr doping can be envisaged; 2) the bilayer $CaCuO_2/CaTiO_3$, that is, with $CaTiO_3$ (CTO) instead of $SrTiO_3$, and thus with no possibility of Ca/Sr interdiffusion, is also superconducting with similar T_c, as shown in Fig.1a. In this case the interface is CuO_2-Ca-TiO_2-CaO (Fig.1d), so identical to the α interface in NGO/CCO/STO but with Ca instead of Sr. As expected, the bilayer NGO/CTO/CCO (not shown) is not superconducting, since, as in NGO/STO/CCO, a β-like interface occurs. This result is important since it generalizes the choice of the non-cuprate block to insulating ABO_3 perovkites other than STO. In particular, among all possible perovkites, the ones yielding superconducting CCO/ABO_3 heterostructures might be the ones for which the corresponding $CaBO_3$ compound exists in form of film.

Apart from the Ca diffusion in the STO, which can be also due to resputtering of light cations during ion-mill thinning, the CCO/STO interface is fairly sharp from the point of view of the other cations. Indeed, in the elemental profile (see Fig. 2h), Cu and Ti profiles decay much faster than the Ca profile, indicating that the CuO_2 plane below the interface is ideal. Moreover, the peak positions in the line profiles in panel h confirm the assumed CuO_2-Ca-TiO_2-SrO plane stacking.

The same measurements were conducted on the STO/CCO β interface (TiO_2-SrO-CuO_2-Ca) taken on the trilayer NGO/STO/CCO/STO [14], showing that all the stoichiometric oxygen ions are present in the interface SrO plane, whereas excess oxygen ions are absent in the Ca plane just above, so that this interface is not conducting (see more details in Supplemental Information [14]).

To estimate how far from the CCO/STO interface the holes, introduced by the extra oxygen ions, diffuse within the CCO layer, we performed oxygen (O) K-edge EELS measurements on several bilayers and trilayers. Indeed, it has been shown that O K-edge X-Ray Absorption Spectroscopy [17,18] and O K-edge EELS [19,20] can reveal the presence of delocalized holes in HTS. In fact a pre-edge feature emerges upon doping HTS, which can be associated to the low-energy quasi-particle band called Zhang-Rice singlet: a locally bound d^9 copper 3d hole hybridized with a doped ligand hole distributed on the planar oxygen 2p orbitals. Thanks to the atomic spatial resolution of STEM/EELS, O K-edge spectra could be acquired across the two types of interfaces with sub-angstrom steps. In

panels a), b) and c) of Fig. 3, the O K-edge spectra acquired in the STO layer and close to the α and β interface of a trilayer NGO/STO/CCO/STO are shown [14]. In the vicinity of interface α, the CCO spectrum shows an additional spectral feature, named A, around 529 eV. This peak disappears on going towards the other interface β and is absent in STO, which is an insulator. According to previous XAS and EELS measurements [17-20], this spectral weight is ascribed to delocalized doping holes. Namely, peak A results mainly from $3d^9\underline{L} \rightarrow 1s3d^{10}$ transitions, where $\underline{L}$ and 1s denote the O $2p_{x,y}$ ligand hole and O 1s core hole, respectively. Peak A is absent in the EELS spectrum of CCO taken far from the interface (Fig. 3c) and in the XAS and EELS spectra of all the insulating parents of high-T_c cuprates [17-20]. In these compounds, the lowest energy peak, usually labeled as "B", occurrs at about 1-2 eV above peak A and is associated with the upper Hubbard band, specifically with the transitions from O 1s orbitals to O 2p orbitals hybridized with Cu 3d orbitals.

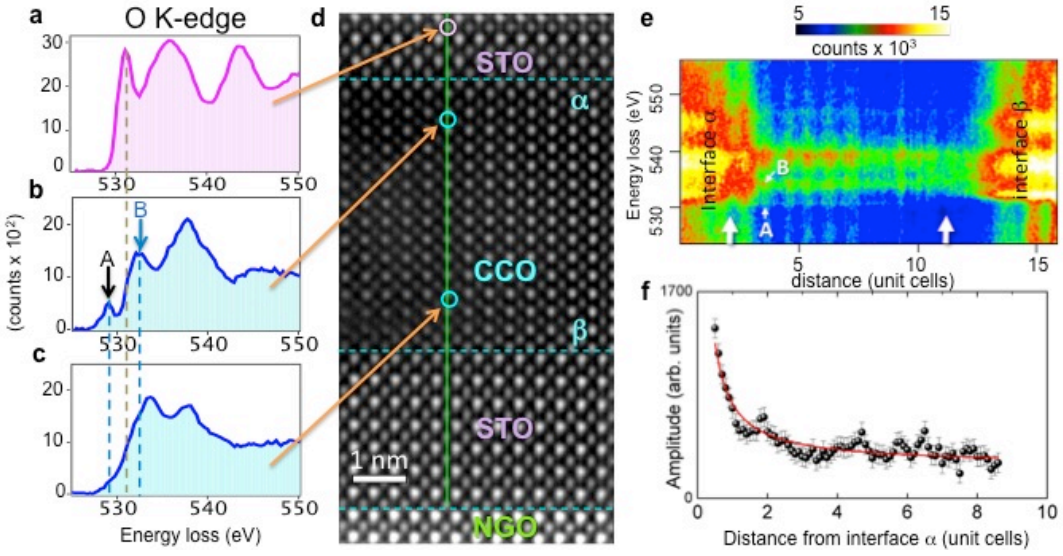

Figure 3: O K-edge measurements in the trilayer NGO/STO/CCO/STO: a) O K-edge from the upper STO layer in (d). b) O K-edge from the CCO close to interface α. c) CCO O K-edge close to interface β. d) HAADF image of the trilayer from which the spectrum image in (e) was taken. e) spectrum image (raw data) showing decreasing peak A amplitude in going from interface α to interface β (big white arrows indicate the range of data shown in f, small white arrows indicate the position of peak A and B as indicated in panel b). f) amplitude of A as a function of the distance *d* from the α interface. The line is a fit with 1/*d* dependence.

In CCO, peak B is mostly masked by the leading edge of higher energy peaks and can only be

resolved in high energy-resolution measurements after background removal [17]. Given the relatively low energy resolution of our EELS measurements [14], the peak visible above A is in fact a convolution of the above mentioned upper Hubbard band peak ($3d^9 \rightarrow 1s3d^{10}$), and other stronger features originating from the overlap of Ca wavefunctions with O p-like states [14]. The dependence of the amplitude of peak A on the distance d from the top interface α is reported in panel f) of Fig. 3. The holes concentration decays rapidly with d and is drastically reduced already in the second CCO unit cell (second CuO_2 plane). This behavior, with $1/d$ dependence, as shown by the fit in Fig.3f, can be explained by the presence of an attractive electrostatic potential [21] associated with the negatively charged extra apical oxygen ions localized at the Ca interface plane.

We can consider the results shown in Fig.3 a *direct* measurement of the detailed dependence of the holes concentration on the number of CuO_2 planes in the IL block of HTS. From this point of view, the dependence of T_c on the number n of CuO_2 planes in multilayered HTS [21-27], where the CR blocks inject carriers from both the top IL/CR and the bottom CR/IL interface, can be explained. Given the dependence of the holes concentration on the distance from the interface shown in Fig. 3, the doping of the CuO_2 planes in HTS with $n \approx 3$ is homogeneous among the planes and the T_c is maximum. For $n > 3$, the holes diffuse also to inner CuO_2 planes, the doping starts to be lower on average and not homogeneous, and the T_c decreases. For $n \geq 4$-5, since the holes are confined by the electrostatic shielding within about 1-2 CuO_2 planes close to each interface of the IL block with the CR block, the inner planes are actually less than underdoped, and, most probably, antiferromagnetic, as also suggested in previous NMR studies [21]. Therefore, the increase of n above 5 should not induce any change in T_c, which, indeed, keeps constant [27]. It is significant that for CCO/STO superlattices a T_c vs. n behaviour identical to the one found in HTS is reported [6]. This fact supports the reliability of the similitude between CCO/STO interface and IL/CR native interface in HTS.

In conclusion, we have shown that the CCO/STO heterostructure with a single interface is superconducting with high T_c. The hole doping of the CuO_2 planes is achieved thanks to extra oxygen atoms, which, during the growth, are incorporated in the Ca plane of CCO at the interface with STO, giving rise to CaO_x composition. A direct measurement of the concentration of the holes as a function

of the distance from the charge reservoir interface shows that they are confined within about 1-2 CCO unit cells. Deeper CuO_2 planes cannot be doped. The same behavior is expected to occur in standard multilayer HTS, where both the IL/CR interfaces are active, thus explaining the dependence of T_c on the number of CuO_2 planes in these systems.

This work also shows that it is possible, in a relatively easy way, to isolate a single CuO_2 high T_c superconducting plane. This is considered an important step towards the achievement of resistance-free electrical transport in 2D channels [28]. Indeed, this is connected to the possibility to realize new superconducting field effect devices, operating at temperatures much higher than the one realized with the LAO/STO heterostructure [9].

Acknowledgement.

DDC whish to acknowledge the help of D. Innocenti at the early stage of this research project. This work was partially supported by Italian MIUR (PRIN Project 2010-2011 OXIDE, "OXide Interfaces: emerging new properties, multifunc-tionality, and Devices for Electronics and Energy". CC was supported by the U.S. Department of Energy, Office of Science, Basic Energy Sciences, Materials Sciences and Engineering Division.

References

[1] H. Y. Hwang, *Mater. Res. Soc. Bull.* **31**, 28–35 (2006).

[2] A. H. Ohtomo, H.Y. Wang, *Nature* **427**, 423 (2004).

[3] A. Tsukazaki *et al., Science* **315,** 1388 (2007).

[4] N. Reyren *et al., Science* **317**, 1196-1199 (2007).

[5] A. Gozar *et al., Nature* **455,** 782 (2008).

[6] D. Di Castro *et al., Phys. Rev. B* **86**, 134524 (2012)

[7] J. E. Kleibeuker *et al., Phys. Rev. Lett.* **113**, 237402 (2014).

[8] R. Pentcheva *et al., Phys. Rev. Lett.* **104**, 166804 (2010).

[9] A. D. Caviglia *et al., Nature* **456**, 624 (2008).

[10] D. Di Castro *et al. Supercond. Sci. Technol.* **27,** 044016 (2014)

[11] G. Balestrino *et al., J. Mater. Chem.* **5**, 1879 (1995).

[12] G. Balestrino, S. Martellucci, P. G. Medaglia, A. Paoletti, and G. Petrocelli, *Phys. Rev. B* **58**, R8925 (1998)

[13] C. Aruta *et al., Phys. Rev. B* **78**, 205120 (2008).

[14] See Supplemental Material [*URL will be inserted by publisher*], which includes Refs. [29-39]

[15] C. Aruta *et al.*, *Phys. Rev. B* **87**, 155145 (2013)

[16] M. Salvato *et al. J. Phys.: Condens. Matter* **25,** 335702 (2013)

[17] T. Chen *et al., Phys. Rev. Lett.* **66**, 104 (1991)

[18] C. T. Chen, *Phys. Rev. Lett.* **68**, 2543 (1992).

[19] H. Romberg, M. Alexander, N. Nucker, P. Adelmann, and J. Fink, *Phys. Rev. B* **42**, 8768R (1990)

[20] N. Gauquelin *et al.*, *Nature Communications* **5**, 4275 (2014)

[21] H. Kotegawa, *J. Phys. Chem. Solids* **62**, 171 (2001).

[22] B. A. Scott *et al., Physica C* **230**, 239–245 (1994).

[23] Y. Tokunaga *et al., J. Low Temp. Phys.* **117,** 473 (1999).

[24] Y. Tokunaga *et al., Phys. Rev. B* **61,** 9707 (2000).

[25] N. Hamada, H. Ihara, *Physica C* **357–360** 108 (2001).

[26] S. Chakravarty, H-Y Kee, K. Voelker, *Nature* **428**, 53 (2004)

[27] A. Iyo *et al., Physica C* **445 -448**, 17-22 (2006)

[28] S. Gariglio, M. Gabay, J-M. Triscone, *Nature nanotechnology* **5**, 13 (2010)

[29] T. Ohnishi *et al*., *Appl. Phys. Lett.* **74**, 2531 (1999).

[30] O.L. Krivanek *et al*., *Ultramicroscopy* **108,** 179 (2008)

[31] N. Dellby *et al., Eur. Phys. J-Appl. Phys.* **54**, 33505 (2011).

[32] S. D. Findlay *et al*., *Appl. Phys. Lett.* **95**, 191913 (2009)

[33] E. Okunishi, H. Sawada, Y. Kondo, *Micron* **43,** 538–544 (2012)

[34] D. Fuchs *at al*., *Journal of Applied Physics* **112**, 103529 (2012)

[35] Guo-zhen Zhu, Guillaume Radtke & Gianluigi A. Botton, *Nature* **490**, 384–387 (2012)

[36] A. Koehl *et al. Phys. Chem. Chem. Phys.* **15**, 8311 (2013)

[37] C. Aruta *et al. Phys. Rev. B* **73**, 235121 (2006)

[38] M. S. Hybertsen *et al. Phys. Rev. B* **45**, 10032 (1992)

[39] H. Romberg *et al. Phys. Rev. B* **42**, 8768 (1990).